PERGAMON

Solid State Communications 113 (2000) 411–414

solid state communications

www.elsevier.com/locate/ssc

Spin–orbit splitting in diamond: excitons and acceptor related states

J. Serrano[1,*], M. Cardona, T. Ruf

Max-Planck-Institut für Festkörperforschung, Heisenbergstr. 1, D-70569 Stuttgart, Germany

Received 15 October 1999; accepted 20 October 1999 by J. Kuhl

Abstract

The spin–orbit splitting $\Delta_0 = 13$ meV calculated ab initio for the Γ_8^+ valence band state of diamond differs from that observed for acceptors ($\simeq$2 meV) and exciton states ($\simeq$7 meV). A full-zone $\mathbf{k}\cdot\mathbf{p}$ band structure, together with a Slater–Koster attractive potential, is used to explain these differences and thus clarify the contradictory assignments of spin–orbit splittings found in the literature for diamond. © 2000 Elsevier Science Ltd. All rights reserved.

Keywords: C. Impurities in semiconductors; D. Spin–orbit effects; E. Inelastic light scattering

Contrary to the case of other tetrahedral semiconductors, no generally accepted experimental information is available for the spin–orbit splitting of the $\Gamma_{25'}^+$ valence states of diamond. Ab initio band structure calculations yield the value $\Delta_0 = 13$ meV[2] [1,2] making the only reported experimental result of 6 meV [3][3] rather dubious. In this letter we discuss the seemingly discrepant values of spin–orbit splittings found in the literature for excitons (7 meV, [4]), acceptor states (2 meV [5] see also Refs. [6,7]), and excitons bound to them (12 meV [4]). We interpret these values by means of a calculation of acceptor levels and exciton binding energies which uses a full-zone $\mathbf{k}\cdot\mathbf{p}$ band structure [8] and a Slater–Koster potential [9]. We conclude that the Δ_0 splitting of the $\Gamma_{25'}^+$ band states is indeed 13 meV while the corresponding ground state of the boron acceptor has a splitting of only 2 meV, the reduction being due to angular momentum quenching by the spread in wavevector induced by the impurity potential. The exciton calculation confirms that the measured splitting of the free exciton is 7 meV. We found no obvious way of relating to spin–orbit coupling the splitting of 12 meV observed for the exciton bound to neutral acceptors [4,10].

The electronic states of acceptors in tetrahedral semiconductors are usually calculated by solving four coupled linear differential equations based on the 4×4 Γ_8^+ Kohn–Luttinger effective mass Hamiltonian [11]. This method assumes that the valence bands are parabolic for a given $\mathbf{k}$-direction and neglects coupling to the Γ_7^+ spin–orbit-split band, thus yielding no information about Γ_7-like spin–orbit-split acceptor states.[4] If Δ_0 is larger than the binding energy of the acceptor ground state, E_b^a, a splitting of this state into a Γ_8 quadruplet and a Γ_7 doublet is expected (we designate the energy splitting by Δ_0^a). Such splittings have been calculated for Si:B within a 6×6 Luttinger–Kohn formalism, treating the Γ_7^+ bands by perturbation theory [12]. The authors of Ref. [12] show that $\Delta_0^a \simeq 1/2\Delta_0$ when $E_b^a \simeq \Delta_0$. In the case of the boron acceptor in diamond, $E_b^a \simeq$ 370 meV is much larger than $\Delta_0(\simeq 13$ meV) and the 6×6 Luttinger–Kohn Hamiltonian should break down. An exact calculation using a screened Coulomb potential is expected to be mathematically very complex and would possibly lack

* Corresponding author.

E-mail address: jserrano@cardix.mpi-stuttgart.mpg.de (J. Serrano).

[1] On leave from University of Valladolid (Spain).

[2] Note that the splitting calculated for the free carbon atom is 11 meV, see Ref. [2]. A renormalization of this value by a factor of 1.2, required also for silicon, confirms the value of 13 meV given in Ref. [1] for diamond.

[3] No justification for the assignment to Δ_0 of structure seen in IR-induced cyclotron resonance is given in this work.

[4] While Γ_8^+ and Γ_7^+ is used for band states, for the corresponding substitutional acceptor states, we use Γ_8 and Γ_7 since inversion symmetry does not hold.

PII: S0038-1098(99)00491-3

Table 1
Parameters used in the **k·p** Hamiltonian. They were taken from Ref. [1] unless otherwise specified

	(eV)		(a.u.)
$E_{\Gamma_1^{+v}}$	−23.00	P	0.538
$E_{\Gamma_{25'}^{+v}}$	0.00	Q	0.780[a]
$E_{\Gamma_{15}^{-c}}$	7.30	R	0.690[a]
$E_{\Gamma_{2'1}^{-c}}$	15.30	P'	−0.300[a]
$E_{\Gamma_{12'}^{-c}}$	26.33	P''	0.076[b]
$E_{\Gamma_1^{+c}}$	24.00	P'''	1.060[a]
$E_{\Gamma_{2'u}^{-c}}$	31.23[b]	Q'	−0.614[b]
$E_{\Gamma_{25'}^{-c}}$	32.49	R'	0.921[b]
Δ_0	0.013	T	0.150[a]
Δ_0'	0.012	T'	0.750[b]

[a] Modified from those in Ref. [1] so as to fit the LMTO band structure corrected for the "gap problem".
[b] Data rescaled from those of Si given in Ref. [8].

physical transparency. We have therefore chosen a simpler Slater–Koster potential (i.e. a finite interaction V_0 when the hole and the impurity are in the cell, zero otherwise; it corresponds to a constant potential in **k**-space). This potential has been successfully used to interpret deep donor levels in III–V compounds [13,14]. E_b^a is obtained by solving the equation

$$\frac{1}{V_0} = G_r(E_b) \tag{1}$$

where G_r is the real part of the Green function of the valence states that have the desired symmetry (either Γ_8 or Γ_7). The potential V_0 can be fixed so as to reproduce, using Eq. (1), the E_b^a measured for the Γ_8 states. Taking the same value of

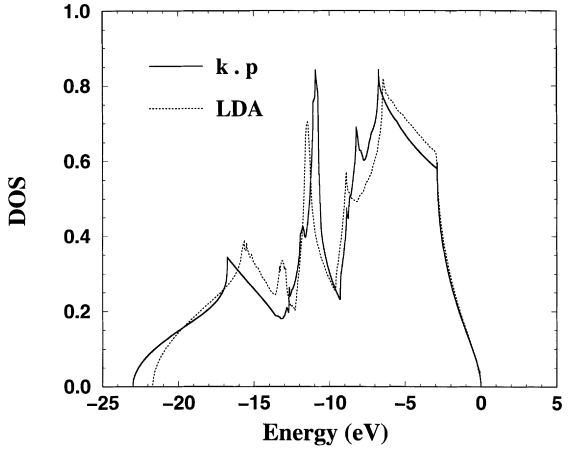

Fig. 1. Total density of valence states calculated for diamond with the 30 × 30 **k·p** Hamiltonian, and the LDA-pseudopotential technique, using a Troullier–Martins pseudopotential [16] and a plane-wave expansion with a cutoff energy of 70 Ry and a grid of 16 × 16 × 16 in reciprocal space.

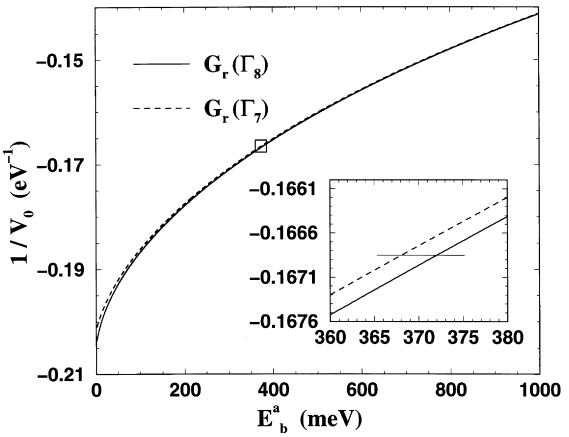

Fig. 2. Real part of the Green function of the valence bands of diamond (labelled $1/V_0$ on the basis of Eq. (1)) vs. E_b^a. The inset represents a blow-up of the rectangle drawn around the binding energy of the boron acceptor. It allows one to see $G_r(\Gamma_8)$ and $G_r(\Gamma_7)$ separately and to determine Δ_0^a vs. E_b^a as illustrated by the horizontal line in the inset (see also Fig. 3).

V_0 for the Γ_7 states, the splitting $\Delta_0^a = E_b(\Gamma_8) - E_b(\Gamma_7)$ is found, without adjustable parameters, provided G_r is known.

We calculate $G_r(\Gamma_8)$ and $G_r(\Gamma_7)$ by a Hilbert transformation of the density of states obtained from the 30 × 30 full-zone **k·p** Hamiltonian including the Γ_8^+, Γ_8^-, Γ_7^+ and Γ_7^- admixture coefficients given by the **k·p** wavefunctions. As **k·p** parameters we used those found in Ref. [1] (based on the fit to an ab initio calculation) with some minor modifications. The full set of parameters employed is displayed in Table 1.

The total density of states obtained with the 30 × 30 **k·p** Hamiltonian is plotted in Fig. 1 together with an LDA pseudopotential calculation using the experimental lattice parameter and the Ceperly–Alder parametrization for the exchange-correlation term [15] (for more details see caption in Fig. 1). Although these LDA results lack accuracy in the energy position of the features because of the so-called "gap problem", the agreement between both calculations is remarkably good.

The projected densities of states $N_v(\Gamma_8)$ and $N_v(\Gamma_7)$ (related to the imaginary part of the Green functions through $N_v(\Gamma_8) = -\pi^{-1}G_i(\Gamma_8)$ and $N_v(\Gamma_7) = -\pi^{-1}G_i(\Gamma_7)$) are calculated with the tetrahedron method using 3×10^5 tetrahedra within the reduced Brillouin zone. The contribution of each tetrahedron to the N_v's is multiplied by the sum of the **k·p** expansion coefficients of the wavefunctions that have the appropriate symmetry (Γ_8 or Γ_7) and added up to obtain the whole projected density of states vs. valence band energy, ω_v. The Hilbert transform leading to $G_r(\Gamma_8)$ and $G_r(\Gamma_7)$ is then calculated numerically by integration over the whole range of ω_v.

Fig. 2 shows $G_r(\Gamma_8)$ and $G_r(\Gamma_7)$ calculated for the valence bands of diamond as described above. The ordinate is

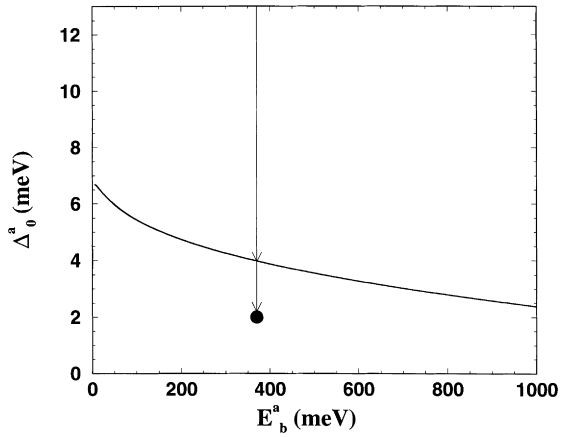

Fig. 3. Spin–orbit splitting Δ^0_a of a substitutional acceptor in diamond vs. binding energy E^a_b calculated as described in the text. The point represents the value measured for a B-acceptor [10]. While theory and experiment differ by a factor of two, agreement becomes more satisfactory when looking at the data in terms of the quenching of the $\Gamma^+_8 - \Gamma^+_7$ band splitting (calculated quenching: 9 meV, measured: 11 meV, as indicated by the vertical arrow).

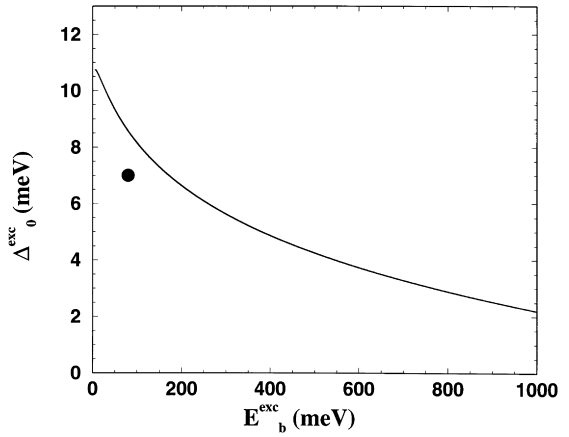

Fig. 5. Spin–orbit splitting of the free edge exciton of diamond vs. binding energy, E^{exc}_b, calculated as described in the text. The point corresponds to the experimental value [4].

labelled $1/V_0$ and the abscissa E^a_b, as corresponds to Eq. (1). The area around the binding energy of the substitutional boron acceptor is shown by the rectangle and corresponds to $V_0 = 6$ eV, a reasonable value for the Slater–Koster potential in diamond. The inset displays a blowup of this rectangle in which $G_r(\Gamma_8)$ and $G_r(\Gamma_7)$ can be seen separately. From this construction, and taking $V_0(\Gamma_8) = V_0(\Gamma_7)$, we find the acceptor level splitting $\Delta^a_0 \simeq 3.9$ meV. This value is nearly twice as large as the measured one [5–7]. We must, however, keep in mind that Δ^a_0 results from a quenching of the band splitting $\Delta_0 = 13$ meV. This calculated quenching is $13 - 4 = 9$ meV while the experimental one is $13 - 2 = 11$ meV. Looking at it this way, the agreement between our simple calculation and the experimental value is satisfactory. In order to illustrate the dependence of Δ^a_0 on E^a_b, we plot in Fig. 3 results obtained with the construction described above in the 0–1 eV range. We have added to this figure the value of 2 meV measured for the B acceptor.

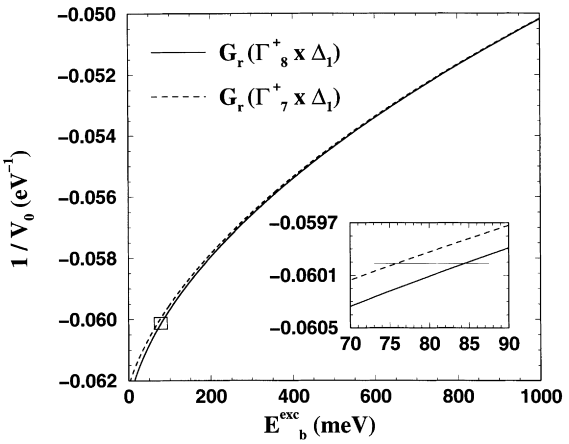

Fig. 4. Real part of the Green function of the exciton bands, corresponding to the product of the $(\Gamma^{+v}_8, \Gamma^{+v}_7)$ and Δ_1, of the valence and conduction bands, respectively. The inset shows a blow-up of the free exciton binding energy and allows to calculate Δ^{exc}_0 as a function of E^{exc}_b (see horizontal line).

A spin–orbit splitting of 7 meV has been observed for the indirect exciton by means of cathodoluminescence [4]. We have estimated this splitting vs. exciton binding energy, E^{exc}_b ($E^{exc}_b \simeq 80$ meV in diamond), with a method similar to that described above for E^a_b, using instead of the valence band energies all possible differences in energies between the conduction and the valence bands. We must, however, take into account the indirect nature of the exciton arising from the fact that the lowest conduction band minima are along the {100} directions, close to the X-points and the corresponding optical transitions at $T = 0$ K must be aided by phonon emission. Therefore we must shift the conduction bands in **k**-space so as to bring one of the Δ minima to $\mathbf{k} = 0$ before performing the calculation. This shift makes it necessary to use a tetragonal instead of the cubic reduced Brillouin zone, thus increasing the number of required sampling points of **k**-space by a factor of 6. The "tetragonal" nature of the indirect gap should also result in a small splitting of the Γ^+_8 valence band exciton which is neglected here ($\simeq$1 meV is obtained from the expressions in Ref. [17]).

Fig. 4 shows the projected G_r calculated for the exciton using as an abscissa the energy difference to the lowest interband gap, i.e. in the spirit of Eq. (1) the exciton binding energy E^{exc}_b. In order to simplify the numerically cumbersome calculation, we have only included the six upper valence bands and the six lowest conduction bands; we have estimated this choice to be sufficient in view of the

small measured value of E_b^{exc} (80 meV). The integral corresponding to Eq. (1) was cut off at 45 eV. We used for the admixture coefficients those of either Γ_8 or Γ_7 valence states and Δ_1 for the conduction bands. This Δ_1 projector is the sum of the coefficients associated with the Γ_1^{+v}, Γ_1^{+c}, and $\Gamma_{15}^{-c}(z)$. Another possibility is to use $\Delta_{2'}$ states (corresponding to $\Gamma_{2'l}^{-c}$, $\Gamma_{2'u}^{-c}$, $\Gamma_{25'}^{+v}$ and $\Gamma_{25'}^{+c}$), but in this case G_r becomes very small and the bound state, in the sense of Eq. (1), appears above the indirect gap, i.e. becomes a band resonance. We thus obtain, by this procedure, two excitons corresponding to a product of (Γ_8^{+v}, Γ_7^{+v}) and Δ_1 states. The spin–orbit splitting Δ_0^{exc} induced by Δ_0 is found to be $\simeq$8.6 meV from Fig. 5, using $E_b^{exc} = 80$ meV. This is in reasonable agreement with the experimental value of 7 meV.

In conclusion, we have performed a systematic calculation of the spin–orbit splittings of acceptors (Δ_0^a) and indirect excitons (Δ_0^{exc}) in diamond, based on a full-zone $\mathbf{k}\cdot\mathbf{p}$ band structure and a Slater–Koster potential. The calculated values agree semiquantitatively with experimental ones, especially when the comparison is performed for $\Delta_0 - \Delta_0^a$ and $\Delta_0 - \Delta_0^{exc}$. The rich fine structure of the D_0 and D_0' lines found for excitons bound to neutral boron [10] cannot be understood within our model, although one of the observed splittings, by about 2 meV, could be attributed to Δ_0^a. The splitting of 12 meV between all components of the D_0 and D_0' lines [4,10], despite being rather close to the spin–orbit coupling value at the band edge, seems to defy the arguments underlying the present approach (an even smaller splitting would be expected, according to Fig. 5, due to the larger sum of acceptor plus exciton binding energy). It is therefore likely that other effects or interactions have to be invoked for their explanation. Similar work for acceptors in silicon will be reported elsewhere [18].

Acknowledgements

We would like to thank V.I. Belitsky for help in the early stages of this work, T.R. Anthony, A.K. Ramdas and R. Sussmann for stimulating discussions. Thanks are also due to D. Olguin, to A. Romero for computational help and to J. Weber for a critical reading of the manuscript. J.S. acknowledges support from Max-Planck-Gesellschaft and Ministerio de Educación y Ciencia (Spain) through the Plan Nacional de Formación del Personal Investigador.

References

[1] M. Willatzen, M. Cardona, N.E. Christensen, Phys. Rev. B 50 (1994) 18054.
[2] F. Herman, S. Skillman, Atomic Structure Calculations, Prentice Hall, Englewood Cliffs, NJ, 1963, p. 2–6.
[3] C.J. Rauch, in: A.C. Stickland (Ed.), Proceedings of the International Conference on the Physics of Semiconductors, Exeter, 1962 (The Institute of Physics and the Physical Society), London, 1962, p. 276.
[4] P.J. Dean, E.C. Lightowlers, D.R. Wight, Phys. Rev. 140 (1965) A352.
[5] E.C. Lightowlers, A.T. Collins, J. Phys. D: Appl. Phys. 9 (1976) 951.
[6] P.A. Crowther, P.J. Dean, W.F. Sherman, Phys. Rev. 154 (1967) 772.
[7] D.M.S. Bagguley, G. Vella-Coleiro, J. Phys. Soc. Jpn 21 (Suppl.) (1966) 244 Proceedings of the International Conference on the Physics of Semiconductors.
[8] M. Cardona, F.H. Pollak, Phys. Rev. 142 (1966) 530.
[9] G.F. Koster, J.C. Slater, Phys. Rev. 96 (1954) 1208.
[10] H. Sternschulte, S. Wahl, K. Thonke, R. Sauer, T. Ruf, M. Cardona, T.R. Anthony, Mater. Sci. Forum 757 (1997) 258–263.
[11] W. Kohn, in: F. Seitz, D. Turnbull (Eds.), Solid State Physics, 5, Academic Press, New York, 1957, p. 257.
[12] N.O. Lipari, A. Baldereschi, Solid State Commun. 25 (1978) 665.
[13] H.P. Hjalmarson, P. Vogl, D.J. Wolford, J.D. Dow, Phys. Rev. Lett. 44 (1980) 810.
[14] P.Y. Yu, M. Cardona, Fundamentals of Semiconductors, 2nd Edition, Springer, Heidelberg, 1999, p. 173.
[15] D.M. Ceperly, B.J. Alder, Phys. Rev. Lett. 45 (1980) 566.
[16] N. Troullier, J.L. Martins, Phys. Rev. B 43 (1991) 1993.
[17] N.O. Lipari, A. Baldereschi, Phys. Rev. B 3 (1971) 2497.
[18] J. Serrano, A. Wysmolek, T. Ruf, M. Cardona, Proceedings of the 20th International Conference on Defects in Semiconductors, Berekely, July, 1999, Phyica B, in press.